

Perturbative Analysis of Two-Temperature Radiative Shocks with Multiple Cooling Processes

Curtis J. Saxton^{1,2} & Kinwah Wu¹

¹ *Research Centre for Theoretical Astrophysics, School of Physics, University of Sydney, NSW 2006, Australia*

² *Sir Frank Packer Department of Theoretical Physics, School of Physics, University of Sydney, NSW 2006, Australia*

Received:

ABSTRACT

The structure of the hot downstream region below a radiative accretion shock, such as that of an accreting compact object, may oscillate due to a global thermal instability. The oscillatory behaviour depends on the functional forms of the cooling processes, the energy exchanges of electrons and ions in the shock-heated matter, and the boundary conditions. We analyse the stability of a shock with unequal electron and ion temperatures, where the cooling consists of thermal bremsstrahlung radiation which promotes instability, plus a competing process which tends to stabilize the shock. The effect of transverse perturbations is considered also. As an illustration, we study the special case in which the stabilizing cooling process is of order 3/20 in density and 5/2 in temperature, which is an approximation for the effects of cyclotron cooling in magnetic cataclysmic variables. We vary the efficiency of the second cooling process, the strength of the electron-ion exchange and the ratio of electron and ion pressures at the shock, to examine particular effects on the stability properties and frequencies of oscillation modes.

Key words: accretion — shock waves — stars: binaries: close — stars: white dwarfs

1 INTRODUCTION

Depending on the form of cooling processes present, radiative shocks may suffer thermal instabilities. The resulting sequence of oscillatory modes has frequencies and stability properties determined by the functional form of the energy loss terms, the rate of energy exchange between ions and electrons, and the particular boundary conditions of the system. Oscillations modulating the structure of the hot downstream column cause variations in the observable emissions. Radiative shocks in several different astrophysical systems show thermal instability, for example the interactions between supernova shocks and the interstellar medium, and accretion streams onto magnetic and non-magnetic compact objects. Many investigations have considered the stability properties of radiative shocks, either through numerical calculations or perturbative analyses (e.g. Falle 1975, 1981; Langer, Chanmugam & Shaviv 1981, 1982; Chevalier & Imamura 1982; Imamura, Wolff & Durisen 1984; Chanmugam, Langer & Shaviv 1985; Imamura 1985; Bertschinger 1986; Innes, Giddings & Falle 1987a, b; Gaetz, Edgar & Chevalier 1988; Wolff, Gardner & Wood 1989; Imamura & Wolff 1990; Houck & Chevalier 1992; Wu, Chanmugam & Shaviv 1992; Tóth & Draine 1993; Dgani & Soker 1994; Imamura et al. 1996; Saxton, Wu & Pongracic 1997; Saxton et al. 1998).

In accreting white dwarfs the flow meets a stand-off accretion shock where the inwards falling matter is suddenly decelerated to subsonic settling flow. The shock sits above the white dwarf surface at a height determined by the path length of the radiative cooling of the downstream material $x_s \approx \frac{1}{4} v_{\text{ff}} t_{\text{cool}}$, which depends on the free-fall velocity of the white dwarf $v_{\text{ff}} = (2GM_{\text{wd}}/R_{\text{wd}})^{1/2}$, and on the cooling timescale $t_{\text{cool}} \sim k_{\text{B}} T/\Lambda$, where Λ is a radiative cooling loss function. In cataclysmic variables (see Warner 1995), the white dwarf accretes mass from a close red dwarf companion star. Thermal bremsstrahlung cooling is an important cooling process in the post-shock region. In cases where the magnetic field of the white dwarf is strong, ($B_{\text{wd}} \gtrsim 10$ MG), (e.g. Lamb & Masters 1979; King & Lasota 1979), cyclotron radiation provides another important cooling process. These competing processes have different dependences on the local flow variables, and therefore they influence the shock stability and oscillatory behaviour differently.

Langer et al. (1981) carried out time-dependent numerical investigations of accretion onto a white dwarf in a planar geometry. Their results show quasi-periodic oscillations due to thermal instability when the cooling is via bremsstrahlung radiation. In the linear perturbative analysis as in Chevalier & Imamura (1982), the radiative shock with bremsstrahlung cooling was shown to have a stable fundamental mode and unstable overtones. They also investigated other cases with

a power-law cooling function in density ρ and temperature T , $\Lambda \propto \rho^a T^b$, with various choices of the power indices (e.g. $(a, b) = (0.5, 2)$ for bremsstrahlung cooling). These investigations show that radiative shocks where the index b is higher are more strongly stabilized against perturbations.

Bertschinger (1986) studied the effect of placing the radiative shock in a spherical geometry. Again the cooling function was a single power-law of density and temperature. In addition to radial perturbations, transverse perturbations were investigated, which are expressed in terms of a scaled transverse wavenumber in addition to the usual oscillation frequency. The modes that are stable in the purely radial analysis of Chevalier & Imamura (1982) are destabilized in the presence of transverse oscillation, but all modes are stable in the limit of large wavenumber.

The stability of physically extended shocks was studied by Houck & Chevalier (1992) for radial accretion onto compact objects, with a Newtonian gravitational potential. The adiabatic index of the gas and the indices of the single power-law cooling term were varied. In the limit of a non-extended shock envelope their calculations yield the same results as Chevalier & Imamura (1982). However even a slight spherical extension of the post-shock region has an effect on the stability: stabilizing the first and second harmonics but destabilizing the higher order modes.

Physical factors other than the cooling processes and geometry also affect the stability properties of a radiative shock. The effects of mass loss from the sides of the post-shock accretion column were examined by Dgani and Soker (1994) by including a sink term in the mass continuity equation. They found that the transverse leakage has a stabilizing effect in the presence of several single power-law radiative cooling processes, and this stabilization was less effective when the cooling had a lower temperature index. Tóth & Draine (1993) investigated radiative shocks that were subject to thermal instability but were supported by a transverse magnetic field. This magnetic pressure support is decisive in determining the stability properties, rather than the characteristics of the radiative cooling alone.

The consequences of inequality between electron and ion temperatures, and the effect of the energy exchange between these fluid components, was considered by Imamura et al. (1996), with the effects of bremsstrahlung and Compton cooling. Their perturbations included a transverse component, as in Bertschinger (1986), although the geometry of the system was planar. Modes with transverse components were less stable than purely longitudinal equivalents, and the presence of the electron-ion exchange also promoted instability. These new effects were qualitatively similar under different choices of the temperature index of the single cooling process.

In these studies, the usual treatment of the radiative cooling processes was to use an approximate energy loss term that is a single power-law in local fluid properties. In the presence of multiple cooling processes, intermediate power-law indices tend to be used. This is not an adequate treatment for the detailed effects of the competition between cooling processes, which is especially important when one process, such as thermal bremsstrahlung radiation, promotes thermal instability, while another process, such as cyclotron emission, has a stabilizing influence. The complicated competition between such processes must be treated by taking an explicit sum of independent power-law contributions for the respective processes.

Chanmugam et al. (1985) performed numerical calculations of the accretion onto a magnetic white dwarf with a sum of separate bremsstrahlung and cyclotron power-law contributions. When cyclotron cooling was strong, the shock was stabilized against oscillations. Further examinations (Wu et al. 1996) revealed that the stabilizing influence depends on the magnetic field strength. In a weak-field regime ($B \lesssim 10\text{MG}$) the competition of the bremsstrahlung and cyclotron cooling, each dominating in different phases of a two-phase oscillatory cycle, allows the perpetuation of small-amplitude oscillations (Wu et al. 1992).

Hujeirat & Papaloizou (1998) performed one- and two-dimensional numerical calculations to investigate the structure and time-dependent behaviour of accretion onto compact objects in the presence of bremsstrahlung cooling, and with consistent solution of the radiative transport and MHD equations. Magnetic field strengths were investigated up to $\sim 10^{-2}$ times the values found in magnetic cataclysmic variables (mCVs). They found that radiation-matter coupling in the flow below the photosphere reduces the amplitudes of the shock oscillations, but that the oscillations are sensitive to the lower boundary condition. In weak-field cases, latitudinal flows out of the accretion column reduce or suppress oscillations; and in stronger field cases there remains some transverse kinks in the magnetic field near the shock, which tends to suppress oscillations because of the effect found by Tóth & Draine (1993).

A composite cooling function was used in the single-temperature perturbative stability analyses of Saxton et al. (1997) and Saxton et al. (1998). The energy loss term consisted of a sum of terms for thermal bremsstrahlung radiation ($\Lambda_{\text{br}} \propto \rho^2 T^{0.5}$) and a second power-law process with a destabilizing influence ($\Lambda_2 \propto \rho^a T^b$ for $b \gtrsim 1$). The cases considered included that of an effective cyclotron cooling term ($\Lambda_{\text{cy}} \propto \rho^{0.15} T^{2.5}$) appropriate for the conditions and flow geometry of accreting magnetic white dwarfs. The analyses examined effects of different values of the efficiency of the second cooling process, which depends on the magnetic field strength in the cyclotron-cooling case. Increasing the cyclotron cooling strength stabilized each mode monotonically, but this happened in a more fundamentally complicated manner than straightforward comparison of cooling and oscillatory timescales would suggest. The order and manner in which the harmonics stabilized depends on the indices of the second cooling process.

In the paper we generalize the previous work in Saxton et al. (1997) and Saxton et al. (1998) for bremsstrahlung-cyclotron radiative accretion shocks in mCVs, by including the effects of unequal electron and ion temperatures and the possibility of transverse perturbations (for a corrugated shock). The equations for a radiative post-shock accretion flow are presented in section 2 and the terms and formulation of the perturbation analysis are developed in section 3. In section 4 we calculate and interpret the frequency and stability properties of the eigenmodes, and explore the effects of varying the parameters of the two-temperature condition, and the relative strengths of the competing cooling processes. In section 5 we discuss the significance of our results in contrast with previous studies dealing with cases with different physical processes or which were less general. We conclude in section 6.

2 FORMULATION

We assume the adiabatic index $\gamma = 5/3$ for an ideal gas, and the equation of state

$$P = \frac{\rho k_B T}{\mu m_H}, \quad (1)$$

where k_B is the Boltzmann constant, and m_H is the mass of the a hydrogen atom. The time-dependent mass continuity, momentum and energy equations for the planar post-shock accretion flow are:

$$\left(\frac{\partial}{\partial t} + \mathbf{v} \cdot \nabla \right) \rho + \rho (\nabla \cdot \mathbf{v}) = 0, \quad (2)$$

$$\rho \left(\frac{\partial}{\partial t} + \mathbf{v} \cdot \nabla \right) \mathbf{v} + \nabla P = 0, \quad (3)$$

$$\left(\frac{\partial}{\partial t} + \mathbf{v} \cdot \nabla \right) P - \gamma \frac{P}{\rho} \left(\frac{\partial}{\partial t} + \mathbf{v} \cdot \nabla \right) \rho = -(\gamma - 1)\Lambda, \quad (4)$$

$$\left(\frac{\partial}{\partial t} + \mathbf{v} \cdot \nabla \right) P_e - \gamma \frac{P_e}{\rho} \left(\frac{\partial}{\partial t} + \mathbf{v} \cdot \nabla \right) \rho = (\gamma - 1)(\Gamma - \Lambda), \quad (5)$$

where P , P_e , \mathbf{v} and ρ are respectively the total pressure, electron pressure, velocity and density of the stream; Λ is the composite radiative cooling function, and Γ is the electron-ion energy exchange.

$$\Gamma = \frac{4\sqrt{2}\pi e^4 n_e n_i \ln C}{m_e c} \left[\frac{\theta_i - (m_e/m_i)\theta_e}{(\theta_e + \theta_i)^{3/2}} \right] \quad (6)$$

where $\ln C$ is the Coulomb logarithm, c is speed of light, e is the electron charge, $\theta_e = k_B T_e/m_e c^2$ and $\theta_i = k_B T_i/m_i c^2$ are the electron and ion temperatures (see, e.g. Melrose 1986). The electron and ion number densities are $n_e = Z\rho/(Zm_e + m_i)$ and $n_i = \rho/(Zm_e + m_i)$ if the ion charge is Z ($Z = 1$ for completely ionized hydrogen plasma).

Optically thin thermal bremsstrahlung radiation provides one of the two cooling processes present, and the other is taken to be a single power-law cooling term. To simplify the analysis, we express the total cooling function in terms of the bremsstrahlung cooling term and a function expressing its functional form compared with the bremsstrahlung cooling term. The parameter ϵ_s is the efficiency of the second cooling process compared to bremsstrahlung cooling, evaluated at the shock, which depends non-linearly on the white dwarf's magnetic field strength, mass and radius, and the pre-shock density and cross-sectional circumference and area of the accretion flow.

$$\Lambda_T \equiv \Lambda_{\text{br}} + \Lambda_2 = \Lambda_{\text{br}} \left[1 + \epsilon_s \left(\frac{P_e}{P_{e,s}} \right)^\alpha \left(\frac{\rho}{\rho_s} \right)^{-\beta} \right]. \quad (7)$$

where ρ_s and $P_{e,s}$ are the density and electron pressure at the shock, $\Lambda_{\text{br}} = C\rho^2(P_e/\rho)^{1/2}$ and the constant $C = (2\pi k_B/3m_e)^{1/2}(2^5\pi e^6/3hm_e c^3)(\mu/k_B m_p^3)^{1/2}g_B$, with h being the Planck constant, m_e the electron mass, m_p the proton mass, μ the mean molecular weight of the gas and g_B the Gaunt factor (see Rybicki & Lightman 1979). The numerical value of C is 3.9×10^{16} in c.g.s. units, assuming that $\mu = 0.5$ and $g_B \approx 1$. The indices α and β are constants describing the functional form of the second cooling process; they adopt particular values for radiative accretion shocks in different physical contexts, but we retain them as parameters for the sake of the general formulation, until results for mCVs are outlined below. (In general for a cooling function $\Lambda_2 \propto \rho^a T^b$, $\alpha = b - 1/2$ and $\beta = 3/2 - a + b$.)

Expressing the composite cooling function in terms of the bremsstrahlung cooling assures us that the second cooling function goes to zero as the density becomes infinite. Using this form assures us that the stability results depend only on the indices of the cooling function and are insensitive to the implementation of the boundary condition at the white dwarf surface, which becomes unambiguous. Alternatively, the cooling could be stopped at a finite density or temperature, with a softened form of the bremsstrahlung term and a different choice of lower boundary. However this approach is mathematically equivalent to the one we have taken except that the new boundary conditions are less obvious, especially for the perturbed variables.

3 PERTURBATION ANALYSIS

The shock position x_s and velocity v_s are subject to a first-order perturbation (as in Imamura et al. 1996):

$$v_s = v_{s1} e^{iky + \omega t} \quad (8)$$

$$x_s = x_{s0} + x_{s1} e^{iky + \omega t}. \quad (9)$$

with frequency ω and a transverse wavenumber k allowing a transverse component for corrugated oscillation. Subscripts 0 and 1 correspond to the stationary state solution and perturbed quantities respectively. In the stationary solution, the shock is at rest: $v_{s0} = 0$. The longitudinal perturbation of the shock position and velocity are related by $v_{s1} = x_{s1}\omega$. The frequency of

the perturbation is ω , and k is the wavenumber of a transverse component of the perturbation in the y direction. Eigenmodes are labelled by a transverse wavenumber and dimensionless eigenfrequency, which are defined as:

$$\kappa = x_{s0}k \quad (10)$$

$$\delta = \frac{x_{s0}}{v_{\text{ff}}}\omega \quad (11)$$

The eigenfrequency is complex, $\delta = \delta_{\text{R}} + i\delta_{\text{I}}$, where δ_{I} is the oscillatory part proportional to the frequency of the particular mode. Stability is indicated by the sign of the growth/decay term δ_{R} . Positive δ_{R} values indicate instability; negative values indicate stability. The physical scales of the system are v_{ff} the free-fall velocity of the white dwarf, ρ_{a} the accretion density, and x_{s0} the equilibrium shock height. The size of the perturbation is indicated by the parameter $\varepsilon \equiv v_{s1}/v_{\text{ff}}$, and therefore $x_{s1} = \varepsilon x_{s0}/\delta$.

To simplify the calculations, the hydrodynamic quantities are expressed in terms of dimensionless variables, allowing the scales of the system to be removed from later equations. These dimensionless variables are expressed in terms of the stationary solutions and perturbations of the velocity, density, total pressure and electron pressure, varying with position in the accretion column $\xi \equiv x/x_s$. The white dwarf surface is at $\xi = 0$ and the shock is $\xi = 1$.

$$\rho(\xi, y, t) = \rho_{\text{a}} \cdot \zeta_0(\xi) \left(1 + \varepsilon \lambda_{\zeta}(\xi) e^{iky + \omega t}\right) \quad (12)$$

$$\mathbf{v}(\xi, y, t) = -v_{\text{ff}} \cdot \left(\tau_0(\xi) \left(1 + \varepsilon \lambda_{\tau}(\xi) e^{iky + \omega t}\right), \varepsilon \tau_0(\xi) \lambda_y(\xi) e^{iky + \omega t}\right) \quad (13)$$

$$P(\xi, y, t) = \rho_{\text{a}} v_{\text{ff}}^2 \cdot \pi_0(\xi) \left(1 + \varepsilon \lambda_{\pi}(\xi) e^{iky + \omega t}\right) \quad (14)$$

$$P_e(\xi, y, t) = \rho_{\text{a}} v_{\text{ff}}^2 \cdot \pi_{e0}(\xi) \left(1 + \varepsilon \lambda_e(\xi) e^{iky + \omega t}\right). \quad (15)$$

where the complex functions λ_{ζ} , λ_{τ} , λ_y , λ_{π} and λ_e represent the effect of the perturbation on the downstream profiles of density, vertical velocity, transverse velocity, total pressure and electron pressure respectively.

The space and time derivatives of a flow variable f , in a frame following the shock, are given by:

$$\frac{Df}{Dx} \approx \frac{1}{x_{s0}} \cdot \left(1 - \varepsilon \frac{e^{iky + \omega t}}{\delta}\right) \left(\frac{\partial f}{\partial \xi}\right) \quad (16)$$

$$\frac{Df}{Dy} \approx \frac{\partial f}{\partial y} - \frac{1}{x_{s0}} \cdot i\varepsilon \frac{\xi \kappa}{\delta} e^{iky + \omega t} \left(\frac{\partial f}{\partial \xi}\right) \quad (17)$$

$$\frac{Df}{Dt} \approx \frac{\partial f}{\partial t} - \frac{v_{\text{ff}}}{x_{s0}} \cdot \varepsilon \xi e^{iky + \omega t} \left(\frac{\partial f}{\partial \xi}\right). \quad (18)$$

None of the hydrodynamic variables has an explicit dependence on position within the accretion column. These shock-frame derivatives are used to expand the equations for mass, momentum and energy continuity, whence are extracted expressions describing the stationary solution and a set of differential equations for the perturbed variables.

We consider expressions in terms of the dimensionless stationary-solution velocity ($\tau_0 \equiv -v_0/v_{\text{ff}}$) to simplify the form of the equations. The stationary solution is obtained by solving the hydrodynamic equations without the time-dependent terms, and it is completely described by two simple algebraic equations for the density and pressure,

$$\zeta_0 = 1/\tau_0 \quad (19)$$

$$\pi_0 = 1 - \tau_0 \quad (20)$$

plus two differential equations: one for the velocity-position profile and the other for the electron pressure:

$$\frac{d\xi}{d\tau_0} = \frac{\gamma \pi_0 - \tau_0}{\tilde{\Lambda}} \quad (21)$$

$$\frac{d\pi_e}{d\tau_0} = \frac{1}{\tau_0} \left[\left(1 - \frac{\tilde{\Gamma}}{\tilde{\Lambda}}\right) (\gamma \pi_0 - \tau_0) - \gamma \pi_e \right] \quad (22)$$

where

$$\tilde{\Gamma} = (\gamma - 1)(\rho_{\text{a}} v_{\text{ff}}^3 / x_{s0})^{-1} \Gamma = (\gamma - 1) \psi_c \psi_{\text{ei}} \frac{1 - \tau_0 - 2\pi_e}{\sqrt{\tau_0^5 \pi_e^3}} \quad (23)$$

and

$$\tilde{\Lambda} = (\gamma - 1)(\rho_{\text{a}} v_{\text{ff}}^3 / x_{s0})^{-1} \Lambda = (\gamma - 1) \psi_c \sqrt{\frac{\pi_e}{\tau_0^3}} [1 + \epsilon_s f(\tau_0, \pi_e)] \quad (24)$$

are appropriate dimensionless forms of the electron-ion exchange and total cooling function respectively. The parameter ψ_{ei} describes the speed of the electron-ion exchange compared to the cooling; when $\psi_{\text{ei}} \lesssim 1$ the two-temperature treatment is justified; otherwise the system behaves like the single-temperature shock described in Saxton et al. (1998). In physical terms the constants ψ_c and ψ_{ei} are:

$$\psi_c = \frac{x_{s0} \rho_{\text{a}}}{v_{\text{ff}}} \cdot \mathcal{C}, \quad (25)$$

and

$$\psi_{ei} = \frac{1}{v_{\text{ff}}^2} \cdot \frac{(\gamma - 1)}{\mathcal{C}} 4(2\pi)^{1/2} \ln C \left(\frac{e^4 m_e^{1/2}}{m_i^{7/2}} \right) \Upsilon(\sigma_s). \quad (26)$$

and $\Upsilon(\sigma_s) \approx 1$ (see Saxton 1999). The function $f(\tau_0, \pi_e)$ describes the local ratio of the power of the second cooling process relative to the bremsstrahlung emission. It takes the form:

$$f(\tau_0, \pi_e) = \frac{4^{\alpha+\beta}}{3^\alpha} \left(\frac{1 + \sigma_s}{\sigma_s} \right)^\alpha \pi_e^\alpha \tau_0^\beta \quad (27)$$

and $\sigma_s \equiv (P_e/P_i)_s$ is the ratio of electron to ion pressures at the shock surface. Upon substitution of these expressions, (19, 20, 23, 24, 27) the equations for the stationary solution velocity (21) and pressure profiles (22) become:

$$\frac{d\xi}{d\tau_0} = \frac{\gamma - (\gamma + 1)\tau_0}{(\gamma - 1)\psi_c [1 + \epsilon_s f(\tau_0, \pi_e)]} \sqrt{\frac{\tau_0^3}{\pi_e}} \quad (28)$$

$$\frac{d\pi_e}{d\tau_0} = \frac{1}{\tau_0} \left[\left(1 - \frac{\psi_{ei}}{1 + \epsilon_s f(\tau_0, \pi_e)} \frac{1 - \tau_0 - 2\pi_e}{\tau_0 \pi_e^2} \right) (\gamma - (\gamma + 1)\tau_0) - \gamma \pi_e \right] \quad (29)$$

For the case of bremsstrahlung cooling alone ($\epsilon_s = 0$) there exists an analytic solution (Aizu 1973). For the general two-process cooling function it is necessary to carry out a numerical integration.

The hydrodynamic equations expressed in terms of the dimensionless perturbed variables give rise to a set of five coupled complex first-order differential equations, which can be expressed in matrix form as:

$$\begin{bmatrix} -\tau_0 & -\tau_0 & 0 & 0 & 0 \\ 0 & -\tau_0 & 0 & \tau_0 - 1 & 0 \\ 0 & 0 & -\tau_0 & 0 & 0 \\ \gamma\tau_0\pi_0 & 0 & 0 & -\tau_0\pi_0 & 0 \\ \gamma\tau_0\pi_e & 0 & 0 & 0 & -\tau_0\pi_e \end{bmatrix} \begin{bmatrix} \lambda'_\zeta \\ \lambda'_\tau \\ \lambda'_y \\ \lambda'_\pi \\ \lambda'_e \end{bmatrix} = \begin{bmatrix} F_1 \\ F_2 \\ F_3 \\ F_4 \\ F_5 \end{bmatrix} \quad (30)$$

where a prime denotes derivatives in ξ and the functions on the right hand side collect the terms which lack derivatives of the perturbed variables. In general, for a cooling function composed of a sum of several power-law terms, they are:

$$F_1(\tau_0, \pi_e, \xi) = -\xi(\ln \tau_0)' - \delta\lambda_\zeta + i\kappa\tau_0\lambda_y \quad (31)$$

$$F_2(\tau_0, \pi_e, \xi) = -(\delta - \tau_0')\lambda_\tau + \xi(\ln \tau_0)' + \tau_0'\lambda_\zeta - \tau_0'(\lambda_\pi - \lambda_\tau) \quad (32)$$

$$F_3(\tau_0, \pi_e, \xi) = -(\delta - \tau_0')\lambda_y + i\kappa(1 - \tau_0)\lambda_\pi + i\kappa\tau_0'\xi/\delta \quad (33)$$

$$F_4(\tau_0, \pi_e, \xi) = -\pi_0\delta(\lambda_\pi - \gamma\lambda_\zeta) - \tilde{\Lambda} \left[-\frac{3}{2}g_2(\tau_0, \pi_e)\lambda_\zeta + \frac{1}{2}g_1(\tau_0, \pi_e)\lambda_e - \lambda_\tau - \lambda_\pi + \frac{1}{\delta} - \frac{\xi}{\tau_0} \right] \quad (34)$$

$$F_5(\tau_0, \pi_e, \xi) = -\pi_e\delta(\lambda_e - \gamma\lambda_\zeta) - \tilde{\Lambda} \left[-\frac{3}{2}g_2(\tau_0, \pi_e)\lambda_\zeta + \frac{1}{2}g_1(\tau_0, \pi_e)\lambda_e - \lambda_\tau - \lambda_\pi + \frac{1}{\delta} - \frac{\xi}{\tau_0} \right] \\ + \tilde{\Gamma} \left[\frac{5}{2}\lambda_\zeta - \frac{3}{2}\lambda_e + \frac{\pi_0\lambda_\pi - 2\pi_e\lambda_e}{\pi_0 - 2\pi_e} - \lambda_\tau - \lambda_e + \frac{1}{\delta} - \frac{\xi}{\tau_0} \right] \quad (35)$$

where the functions $g_1(\tau_0, \pi_e)$ and $g_2(\tau_0, \pi_e)$ are defined as:

$$g_1(\tau_0, \pi_e) = 1 + \frac{2\epsilon_s\alpha f(\tau_0, \pi_e)}{1 + \epsilon_s f(\tau_0, \pi_e)}, \quad (36)$$

$$g_2(\tau_0, \pi_e) = 1 - \frac{2}{3} \left[\frac{\epsilon_s\beta f(\tau_0, \pi_e)}{1 + \epsilon_s f(\tau_0, \pi_e)} \right], \quad (37)$$

The perturbed transverse velocity variable λ_y has an inconspicuous influence. If not for its presence in the F_1 function, λ_y would be decoupled from the other perturbed variables, and could be integrated separately after finding the solutions in the other variables.

The matrix in (30) is non-singular everywhere in the post-shock region except at $\tau_0 = 0$. In a practice this singularity doesn't matter because the numerical integration can be taken to some small value $\tau_0 = \Delta > 0$ and the results reach a limit as $\Delta \rightarrow 0$. The matrix equation is inverted using (21) to yield equations for the perturbed variables.

$$\frac{d}{d\tau_0} \begin{bmatrix} \lambda_\zeta \\ \lambda_\tau \\ \lambda_y \\ \lambda_\pi \\ \lambda_e \end{bmatrix} = \frac{1}{\tilde{\Lambda}} \begin{bmatrix} 1 & -1 & 0 & 1/\tau_0 & 0 \\ -\gamma\pi_0/\tau_0 & 1 & 0 & -1/\tau_0 & 0 \\ 0 & 0 & -(\gamma\pi_0 - \tau_0)/\tau_0 & 0 & 0 \\ \gamma & -\gamma & 0 & 1/\pi_0 & 0 \\ \gamma & -\gamma & 0 & \gamma/\tau_0 & -(\gamma\pi_0 - \tau_0)/\tau_0\pi_e \end{bmatrix} \begin{bmatrix} F_1 \\ F_2 \\ F_3 \\ F_4 \\ F_5 \end{bmatrix} \quad (38)$$

These resulting differential equations are split into real and imaginary parts to yield ten first-order differential equations in real eigenfunctions, λ_{ζ_R} , λ_{ζ_I} , λ_{τ_R} , λ_{τ_I} , λ_{y_R} , λ_{y_I} , λ_{π_R} , λ_{π_I} , λ_{e_R} , and λ_{e_I} , plus the known parameters and variables of the static solution, α , β , $\xi(\tau_0)$ and $\pi_e(\tau_0)$. This decomposition is straightforward because only the vector parts of (38) are complex.

To obtain the equations for real variables, we substitute the real parts of the λ -variables in the left side and real parts of the F -functions in the right side. Similarly, the equations for the eigenfunctions' imaginary parts are obtained by substituting imaginary parts of the λ -variables and F -functions.

Optically thick cyclotron emission provides an important cooling process for accretion onto strongly magnetic white dwarfs. An optically thick radiative process cannot in general be described by a simple local energy loss function. A full treatment requires simultaneous solution to the time-dependent hydrodynamic and radiative transfer equations. However for the particular geometry of the field-aligned accretion flow in mCVs and the physical conditions typical of such systems, cyclotron radiation is optically thick up to a critical frequency at which it becomes optically thin. The total power escaping from the post-shock region locally in the accretion column approximately takes the form of a power-law cooling term $\Lambda_{\text{cyc}} \propto \rho^{3/20} T_e^{5/2}$, which in the terms of (7) corresponds to indices $\alpha = 2.0$ and $\beta = 3.85$ (see Langer et al. 1982, Wu, Channugam & Shaviv 1994, Cropper et al. 1999). This approximation renders the linear analysis tractable.

For the special case of a mCV radiative shock with bremsstrahlung and cyclotron cooling present, the parameter ϵ_s is related to the magnetic field at the accretion pole. The expression for ϵ_s is as described in Wu (1994). In the single-temperature limit $\sigma_s = 1$, but the value in the two-temperature conditions depends on the conduction of energy upstream of the ion shock, carried by the electrons. Our analysis treats σ_s as a parameter.

4 RESULTS

4.1 Eigen-modes

The ten real differential equations are integrated numerically using a Runge-Kutta method. In terms of the dimensionless perturbed variables, the boundary conditions at the shock are $\tau_0 = 1/4$, $\xi = 1$, $\pi_e = \frac{3}{4}(1 + 1/\sigma_s)^{-1}$, $\lambda_\zeta = 0$, $\lambda_\tau = -3$, $\lambda_y = 3i\kappa/\delta$ and $\lambda_\pi = \lambda_e = 2$. At the dwarf surface ($\tau_0 = 0$, $\xi = 0$, $\pi_e = 1/2$) there are no specific conditions on the values of the perturbed density and pressures, but the stationary wall condition $\lambda_\tau = 0$ applies (see Chevalier & Imamura 1982; Imamura et al. 1996; Saxton et al. 1997). Integration proceeds between $\tau_0 = 0$ and $\tau_0 = 1/4$ for trial values of δ_R and δ_I . Values of the δ 's are sought which yield $\lambda_\tau = 0$ when the differential equations are integrated to $\tau_0 = 0$ (using the search method described in the appendices of Saxton et al. 1998) Each of these eigenvalues corresponds to an oscillatory mode of the shock. The modes form an indefinite sequence consisting of a fundamental mode and a succession of overtones.

The survey of the complex frequency eigenplane is conducted in a region of δ appropriate for the lowest modes. The range of frequency δ_I explored is from 0 to 3.5; the growth/decay term δ_R is taken from 0.4 down to -0.4 or lower if necessary in cases of higher κ . The perturbed velocity eigenfunction is evaluated at the white dwarf surface for each sampled of δ . Values of $-\log |\lambda_\tau|_{\text{wd}}$ are plotted and the maxima of this quantity indicate the δ eigenvalues.

This procedure is performed for single-temperature ($\sigma_s = 1$, large ψ_{ei}) and two-temperature ($\sigma_s \leq 1$, ψ_{ei} finite) cases. Eigenfrequencies of the six lowest modes are calculated under the conditions $\sigma_s = 0.2, 0.5, 1$ and $\psi_{ei} = 0.1, 0.5, 1$ to test the effect of the unequal electron and ion pressures at the shock, and the rate of electron-ion energy exchange in the accretion column. For each case we investigate the modes' frequencies and stability properties under conditions with bremsstrahlung cooling alone ($\epsilon_s = 0$), cyclotron cooling comparable to the bremsstrahlung ($\epsilon_s = 1$), and cyclotron cooling dominant ($\epsilon_s = 100$), as evaluated at the shock surface. These eigenvalues are tabulated in Table 1.

Applying the special restricted choice of the $\epsilon_s = 0$ exactly recovers earlier results of Imamura et al. (1996) for a two-temperature shock with only a single bremsstrahlung cooling process. Taking the limits of high ψ_{ei} and $\sigma_s = 1$ reduces our equations to reproduce the single-temperature case with multiple cooling, as in Saxton et al. (1997). Taking this limit and $\epsilon_s = 0$ together reproduces the single-temperature bremsstrahlung-cooling only results of Chevalier & Imamura (1982).

The frequencies and stability behaviour of the fundamental and first overtone in the presence of the two-temperature conditions and composite cooling was also investigated for non-longitudinal perturbations. This corrugation of the shock is represented by non-zero values of the dimensionless transverse wavenumber κ .

4.2 Frequency quantization

Under the simple conditions, for either bremsstrahlung-dominated cooling or a single-temperature shock, the oscillatory part of the eigenfrequency follows a quantized sequence like the modes of a pipe open at one end. In a linear fit to this sequence, the harmonics n follow $\delta_I \approx \delta_{IO}(n - 1/2) + \delta_C$, with frequency spacing δ_{IO} and a small constant correction offset δ_C . The two-temperature parameters σ_s and ψ_{ei} and the secondary process' cooling efficiency ϵ_s determine the values of these constants. Parameter fits were performed for the first six harmonics under different conditions, and the results for the constant and linear coefficients are shown in Table 2.

For a purely bremsstrahlung-dominated shock the mode spacing $\delta_{IO} \approx 0.6$ regardless of the two-temperature conditions. As ϵ_s is increased under given σ_s and ψ_{ei} conditions, δ_{IO} becomes steadily smaller. For very efficient cyclotron cooling ($\epsilon_s = 100$) the spacing is reduced to $\delta_{IO} \approx 0.3$. The decline of δ_{IO} with increasing ϵ_s is fastest for cases with high ψ_{ei} ; and increasing ψ_{ei} for given (σ_s, ϵ_s) (approaching single-temperature conditions) makes δ_{IO} smaller. In other words, when the electron-ion exchange is weak, the effect of ϵ_s on the mode frequencies is reduced.

The frequency offset constant δ_C increases steadily with increasing ϵ_s for all observed values of the two-temperature and cooling parameters (σ_s, ψ_{ei}). For an increasingly cyclotron-cooling dominated flow in the presence of strong two-temperature

Table 1. Eigenvalues δ_R , δ_I in the absence of transverse perturbation ($\kappa = 0$), for various conditions of electron/ion pressure ratio at the shock (σ_s), strength of electron-ion energy exchange (ψ_{ei}), and relative efficiency of cyclotron cooling (ϵ_s).

σ_s	ψ_{ei}	$\epsilon_s = 0$		$\epsilon_s = 1$		$\epsilon_s = 100$	
0.2	0.1	-0.001	0.307	-0.057	0.343	-0.113	0.335
		0.048	0.902	-0.040	0.808	-0.073	0.567
		0.066	1.529	-0.030	1.363	-0.067	0.978
		0.092	2.141	0.005	1.896	-0.052	1.387
		0.095	2.769	-0.001	2.444	-0.036	1.758
		0.114	3.385	0.027	2.995	-0.046	2.154
0.2	0.5	-0.007	0.306	-0.106	0.340	-0.166	0.247
		0.047	0.894	-0.054	0.758	-0.043	0.528
		0.060	1.513	-0.076	1.272	-0.111	0.775
		0.085	2.120	-0.040	1.756	-0.088	1.104
		0.087	2.739	-0.054	2.253	-0.071	1.406
		0.106	3.349	-0.026	2.770	-0.086	1.710
0.2	1.0	-0.009	0.306	-0.123	0.332	-0.163	0.211
		0.047	0.891	-0.056	0.744	-0.056	0.520
		0.060	1.509	-0.087	1.243	-0.101	0.701
		0.085	2.115	-0.046	1.717	-0.109	1.006
		0.086	2.733	-0.067	2.193	-0.081	1.271
		0.105	3.342	-0.043	2.701	-0.094	1.541
0.5	0.1	0.003	0.304	-0.025	0.322	-0.057	0.309
		0.051	0.898	0.006	0.849	-0.027	0.582
		0.068	1.522	0.020	1.435	-0.014	1.013
		0.093	2.132	0.044	2.002	0.003	1.416
		0.096	2.756	0.044	2.585	0.002	1.819
		0.114	3.370	0.064	3.161	0.008	2.232
0.5	0.5	-0.006	0.306	-0.065	0.332	-0.135	0.264
		0.048	0.892	-0.019	0.823	-0.023	0.551
		0.061	1.511	-0.016	1.389	-0.081	0.868
		0.086	2.117	0.011	1.930	-0.049	1.218
		0.088	2.735	0.006	2.490	-0.051	1.547
		0.107	3.345	0.031	3.047	-0.059	1.906
0.5	1.0	-0.008	0.305	-0.078	0.332	-0.148	0.239
		0.048	0.891	-0.023	0.814	-0.036	0.549
		0.061	1.508	-0.023	1.376	-0.092	0.816
		0.085	2.113	0.006	1.910	-0.073	1.159
		0.087	2.730	-0.002	2.463	-0.064	1.448
		0.106	3.339	0.023	3.015	-0.083	1.781
1.0	0.1	0.010	0.299	-0.001	0.303	0.002	0.277
		0.056	0.892	0.036	0.856	0.027	0.564
		0.071	1.511	0.047	1.447	0.048	0.997
		0.093	2.118	0.064	2.025	0.052	1.378
		0.095	2.735	0.064	2.610	0.043	1.798
		0.112	3.345	0.078	3.192	0.060	2.199
1.0	0.5	-0.005	0.304	-0.039	0.319	-0.096	0.262
		0.049	0.890	0.009	0.846	0.007	0.554
		0.063	1.507	0.019	1.430	-0.032	0.909
		0.087	2.112	0.042	1.995	-0.000	1.257
		0.089	2.729	0.040	2.576	-0.022	1.610
		0.107	3.337	0.061	3.150	-0.014	1.992
1.0	1.0	-0.007	0.305	-0.050	0.322	-0.122	0.247
		0.049	0.890	0.004	0.843	-0.015	0.559
		0.062	1.506	0.012	1.425	-0.059	0.876
		0.086	2.110	0.038	1.988	-0.025	1.230
		0.088	2.727	0.035	2.566	-0.038	1.545
		0.106	3.335	0.056	3.139	-0.046	1.915

Table 2. Mode frequency spacing δ_{IO} and offset δ_{C} for a linear fit $\delta_1 \approx \delta_{\text{IO}}(n - 1/2) + \delta_{\text{C}}$, under different two-temperature conditions $(\sigma_{\text{s}}, \psi_{\text{ei}})$ and efficiency of the second cooling process (ϵ_{s}).

σ_{s}	ψ_{ei}	ϵ_{s}	δ_{IO}	δ_{C}	σ_{s}	ψ_{ei}	ϵ_{s}	δ_{IO}	δ_{C}	σ_{s}	ψ_{ei}	ϵ_{s}	δ_{IO}	δ_{C}
0.2	0.1	0	0.617	-0.013	0.5	0.1	0	0.615	-0.014	1.0	0.1	0	0.610	-0.015
0.2	0.1	1	0.534	0.039	0.5	0.1	1	0.571	0.014	1.0	0.1	1	0.580	0.000
0.2	0.1	100	0.374	0.076	0.5	0.1	100	0.392	0.051	1.0	0.1	100	0.391	0.028
0.2	0.5	0	0.610	-0.010	0.5	0.5	0	0.609	-0.011	1.0	0.5	0	0.608	-0.011
0.2	0.5	1	0.489	0.057	0.5	0.5	1	0.547	0.030	1.0	0.5	1	0.569	0.013
0.2	0.5	100	0.294	0.080	0.5	0.5	100	0.330	0.069	1.0	0.5	100	0.348	0.055
0.2	1.0	0	0.609	-0.011	0.5	1.0	0	0.608	-0.010	1.0	1.0	0	0.608	-0.011
0.2	1.0	1	0.476	0.060	0.5	1.0	1	0.540	0.032	1.0	1.0	1	0.566	0.015
0.2	1.0	100	0.263	0.086	0.5	1.0	100	0.307	0.077	1.0	1.0	100	0.333	0.063

Table 3. Parameters of the frequency spacing for a quadratic fit, $\delta_1 \approx \delta_{\text{Q}}n^2 + \delta_{\text{IO}}(n - 1/2) + \delta_{\text{C}}$, under different two-temperature conditions $(\sigma_{\text{s}}, \psi_{\text{ei}})$ and efficiency of the second cooling process (ϵ_{s}).

σ_{s}	ψ_{ei}	ϵ_{s}	δ_{IO}	δ_{C}	δ_{Q}	σ_{s}	ψ_{ei}	ϵ_{s}	δ_{IO}	δ_{C}	δ_{Q}	σ_{s}	ψ_{ei}	ϵ_{s}	δ_{IO}	δ_{C}	δ_{Q}
0.2	0.1	0	0.604	-0.002	0.002	0.5	0.1	0	0.602	-0.033	0.002	1.0	0.1	0	0.601	0.007	0.001
0.2	0.1	1	0.484	0.080	0.007	0.5	0.1	1	0.541	0.038	0.004	1.0	0.1	1	0.564	0.013	0.002
0.2	0.1	100	0.291	0.144	0.012	0.5	0.1	100	0.319	0.113	0.011	1.0	0.1	100	0.327	0.082	0.009
0.2	0.5	0	0.596	0.001	0.002	0.5	0.5	0	0.595	0.001	0.002	1.0	0.5	0	0.595	0.000	0.002
0.2	0.5	1	0.436	0.102	0.007	0.5	0.5	1	0.508	0.062	0.005	1.0	0.5	1	0.541	0.036	0.004
0.2	0.5	100	0.252	0.115	0.006	0.5	0.5	100	0.279	0.112	0.007	1.0	0.5	100	0.292	0.101	0.008
0.2	1.0	0	0.594	0.002	0.002	0.5	1.0	0	0.594	0.001	0.002	1.0	1.0	0	0.593	0.002	0.002
0.2	1.0	1	0.428	0.100	0.007	0.5	1.0	1	0.501	0.065	0.006	1.0	1.0	1	0.536	0.041	0.004
0.2	1.0	100	0.245	0.100	0.003	0.5	1.0	100	0.282	0.098	0.004	1.0	1.0	100	0.298	0.093	0.005

effects, $\delta_{\text{C}} \rightarrow \frac{1}{2}\delta_{\text{IO}}$, which means that the nature of the modes becomes more analogous to a pipe with two open ends. The increased importance of the two temperature effects in the large ϵ_{s} regime means that the fixed wall boundary condition loses importance and the global stability of the accretion column depends more on the disparity of electron and ion temperatures within the stream than on the radiative cooling processes (cf. Imamura et al. 1996). The frequency and stability properties in this case are determined by the exchange process rather than the radiative cooling.

Better fits are obtained by introducing another parameter describing a quadratic dependence on harmonic number, $\delta_1 \approx \delta_{\text{Q}}n^2 + \delta_{\text{IO}}(n - 1/2) + \delta_{\text{C}}$. This quadratic correction is very small in all examined cases, but its presence affects the values of δ_{IO} and δ_{C} such that $\delta_{\text{C}} \rightarrow \frac{1}{2}\delta_{\text{IO}}$ sooner and more readily in the high- ϵ_{s} cases, as shown in Table 3. With this fit $\delta_{\text{C}} \approx \frac{1}{3}\delta_{\text{IO}}$ by the point of $\epsilon_{\text{s}} = 100$. Without the δ_{Q} term, the sequence of modes approaches the behaviour of a doubly-open pipe much more slowly in ϵ_{s} .

4.3 Stability properties

The most unstable systems investigated are those with bremsstrahlung cooling only ($\epsilon_{\text{s}} = 0$). Varying the values of σ_{s} and ψ_{ei} has little effect in the small- ϵ_{s} extreme, because most of the cooling is due to bremsstrahlung radiation, which occurs in the dense region near the white dwarf surface, where the electron and ions have nearly reached equilibrium regardless of their initial two-temperature conditions close to the shock. For most realistic parameters with low or modest ϵ_{s} , the fundamental mode is stable. The fundamental is unstable only in cases of extremely low ψ_{ei} , modest or high σ_{s} , and low ϵ_{s} . Otherwise the second harmonic is the lowest potentially unstable mode.

Except when cyclotron cooling and two-temperature effects are both very strong (when ψ_{ei} is very small and ϵ_{s} is large), for given conditions of $(\sigma_{\text{s}}, \psi_{\text{ei}})$, increasing ϵ_{s} stabilizes every mode in a monotonic manner. Under these usual conditions a mode which is unstable for some value of ϵ_{s} is also unstable for all cases of lower ϵ_{s} ; and furthermore an increase in ϵ_{s} does not cause a decrease in a mode's stability.

For a given change of ϵ_{s} the stability term δ_{R} of each mode progresses in a way that is individual to the mode and apparently independent of the stability behaviour of the other modes of the sequence. Some modes experience more rapid reduction in δ_{R} for a given increase in ϵ_{s} , therefore they tend to stabilize earlier or quicker than other modes, if all else is equal.

The transition of a particular mode from the unstable ($\delta_{\text{R}} > 0$) to stable ($\delta_{\text{R}} < 0$) regions of the complex frequency

eigenplane occurs at some threshold value of ϵ_s that is individual to the mode and dependent on the (σ_s, ψ_{ei}) conditions. The lowest modes usually stabilize at lower ϵ_s because they tend to be in or closer to the $\delta_R < 0$ region even in the bremsstrahlung-cooling only case. However there often are exceptions, because of the the modes' rates of stabilization, $\partial\delta_R/\partial\epsilon_s$, depend on ϵ_s and are individual to each n . There are many cases of $(\sigma_s, \psi_{ei}, \epsilon_s)$ where a mode n is unstable but a higher mode $n + 1$ is stable. Therefore for some cases of (σ_s, ψ_{ei}) there are modes which can never be the lowest unstable mode for any value of ϵ_s .

It is instructive to examine collectively the stability values δ_R of the sequence of modes at some set of parameters $(\sigma_s, \psi_{ei}, \epsilon_s)$. In the cases of lower ϵ_s there is a general pattern in which each successive harmonic is less stable than the lower neighbouring mode; δ_R increases with harmonic number n . The increases of δ_R between consecutive modes is smaller in the ranges of higher n . As ϵ_s increases this trend weakens, because some modes stabilize fast enough to overtake neighbouring lower modes. When ϵ_s is very high, the modal stability eigenvalues, δ_R , are scattered in a negative range of values, except for the lowest modes which tend to deviate further towards greater or lesser δ_R . The introduction and strengthening of two-temperature effects enhances the departures from the general pattern.

The eigenmodes for various ϵ_s under the one- and two-temperature conditions are compared in Figure 1. Decreasing ψ_{ei} from indefinitely high values (single-temperature flow) to very low values (the two-temperature conditions strong) has little effect on the stability of the modes if bremsstrahlung cooling is the dominant process (ϵ_s is small). In intermediate ranges of ϵ_s , with cyclotron and bremsstrahlung cooling comparable in efficiency, strengthening the two-temperature conditions tends to stabilize most modes. When ϵ_s is very high, the influence of two-temperature effects on the stability of individual modes is pronounced. Introduction of two-temperature effect in high ϵ_s tends to destabilize most modes, and the pattern of variations of δ_R from one mode to the next becomes very different from the one-temperature case. For some (σ_s, ψ_{ei}) , two-temperature effects cause one or more of the lower modes to remain unstable even for very high ϵ_s , or even to destabilize a mode as ϵ_s increases past some threshold.

4.4 Transverse perturbation

The stability properties and frequency behaviour of the oscillatory modes were investigated in the presence of transverse perturbations, under the two-temperature conditions and with explicit competition between bremsstrahlung cooling and the second cooling (cyclotron cooling). The eigenvalues of the fundamental and first overtone were traced through a range of κ for particular choices of $(\sigma_s, \psi_{ei}, \epsilon_s)$.

The special case $\kappa = 0$ is the absence of transverse perturbations in which the oscillatory behaviour is the same as that described in subsections above. In the limit of large κ all of the modes become strongly stable, and the frequencies approach a sequence like a doubly-open pipe, $\delta_1 \propto \delta_{10} n$. Between these extremes, the effect of transverse perturbations on the frequency and stability of the accretion column is specific to each mode. For a given mode with harmonic number n , the interesting behaviour takes place up to a threshold $\kappa \approx 2n + 1$. As κ increases, there is a growing region of the eigenplane within which the modes $n \lesssim (\kappa - 1)/2$ show the simple behaviour like the large- κ extreme. The modes outside the region experience individual and non-simple disturbances as κ is varied, reverting to the standard $\kappa = 0$ behaviour in the large- n modes.

For each mode, the instability term δ_R experiences a number of maxima as κ varies. For a mode with harmonic number n , there are n of these maxima. Increasing ϵ_s affects the values of these maxima in (κ, δ_R) . For low ϵ_s the maxima are most distinct, but one or more maxima may become narrow and shallow almost to the point of vanishing as ϵ_s becomes very large. (See Figure 5, for example.) In the fundamental mode, the single maximum is at about $\kappa \approx 3/2$ for low ϵ_s (see the $\epsilon_s = 0$ restricted case in Imamura et al. 1996) and gradually moves towards lower κ as ϵ_s increases. In the first overtone, there is a maximum at $\kappa = 0$ and another one in the vicinity of $\kappa \sim 1 - 4$. As ϵ_s increases, the former maximum lowers in δ_R and narrows, whilst the second maximum moves to lower κ . When a maximum of instability (other than $\kappa = 0$) migrates to smaller κ with increasing ϵ_s , the tendency is for the peak δ_R to increase until some critical value of ϵ_s is attained, after which the peak δ_R decreases slowly with increasing ϵ_s . These thresholds depend upon n , ψ_{ei} and σ_s . The threshold is less than $\epsilon_s = 100$ when σ_s is small. In instances of very high ϵ_s a mode may be stable for all κ , except when σ_s is large or ψ_{ei} is small. In all cases studied, enormous values of $\epsilon_s \gtrsim 100$ are required to stabilize modes other than the fundamental. For example, the fundamental is stabilized completely by $\epsilon_s = 100$ in Figures 2, 4, but not in Figure 6, where ψ_{ei} is too small.

For all modes under all conditions, the oscillatory frequency δ_1 increases monotonically with κ . In the presence of transverse oscillations, consecutive modes are no longer unique in δ_1 : it is possible for modes n and $n + 1$ to have the same δ_1 but different transverse component κ . However the modes do not become degenerate; there is no case in which different modes have the same κ and δ_1 . For each mode the rise of δ_1 with κ is smooth and is a function of ϵ_s . Typical values of the gradient $\partial\delta_1/\partial\epsilon_s$, for given κ , are greater for higher ϵ_s . For sufficiently high κ and ϵ_s , δ_1 reaches a plateau for each mode. (See the left side of Figures 2-7).

4.5 Summary

We have found:

- (i) When ϵ_s is large, two-temperature effects are very important in determining the frequency and stability properties of the accretion flow; when ϵ_s is small, the two-temperature conditions are ineffectual. Increasing ϵ_s decreases the frequency spacing of the modes. Varying ϵ_s alters the instability of each mode at a rate that depends on the harmonic number n , and

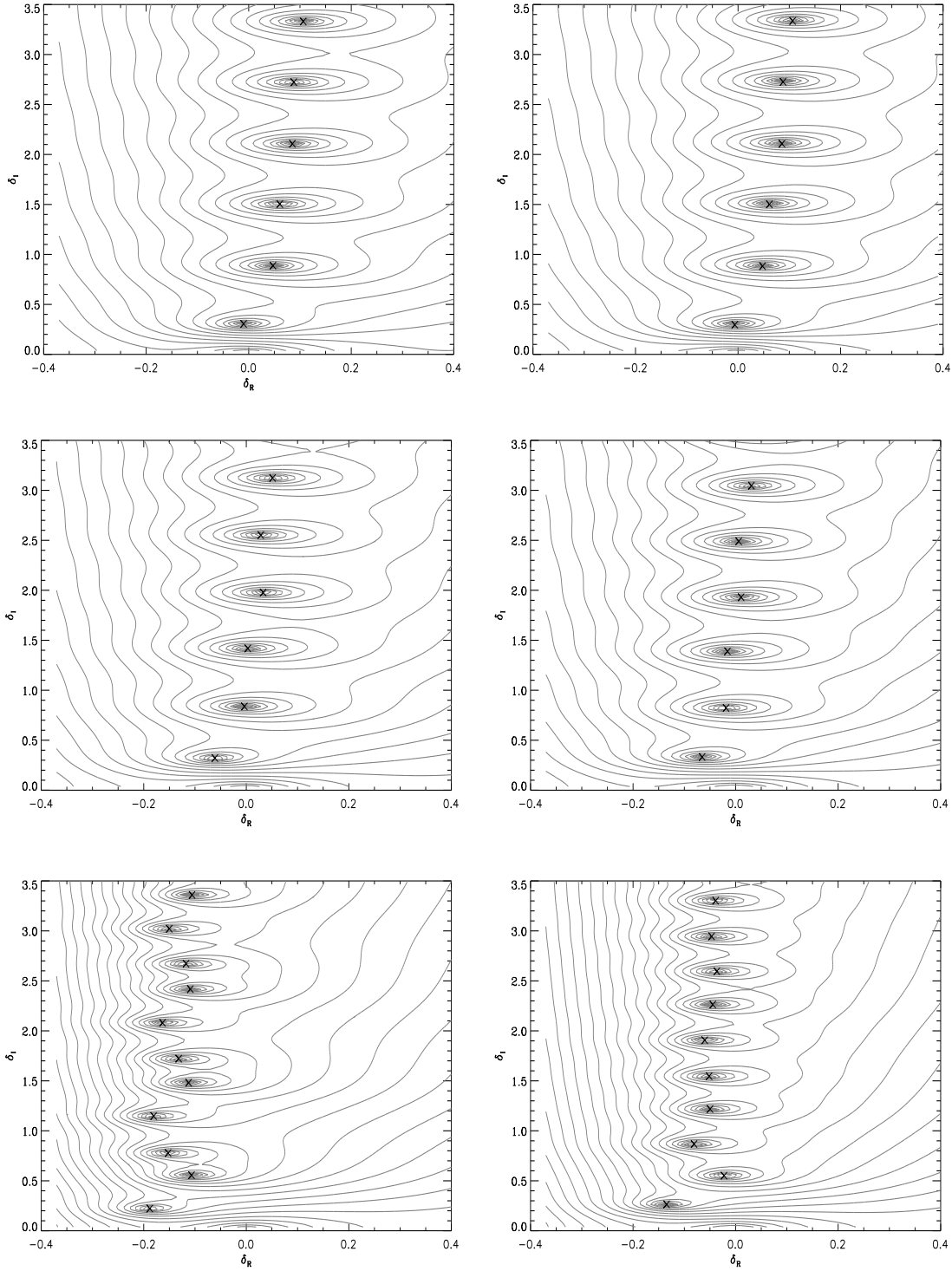


Figure 1. Complex $\delta = \delta_{\text{R}} + i\delta_{\text{I}}$ eigenplanes, with contours of the logarithm of the perturbed velocity eigenfunction evaluated at the white dwarf surface. The modes are the points where the perturbed velocity goes to zero, marked with crosses. The left column represents the one-temperature cases; the right column shows two-temperature cases with $\psi_{\text{ei}} = 0.5$ and $\sigma_{\text{s}} = 0.5$. The top row shows bremsstrahlung-cooling only shocks, with $\epsilon_{\text{s}} = 0$; in the middle row bremsstrahlung and cyclotron cooling are comparable $\epsilon_{\text{s}} = 1$; and in the bottom row cyclotron cooling dominates $\epsilon_{\text{s}} = 100$.

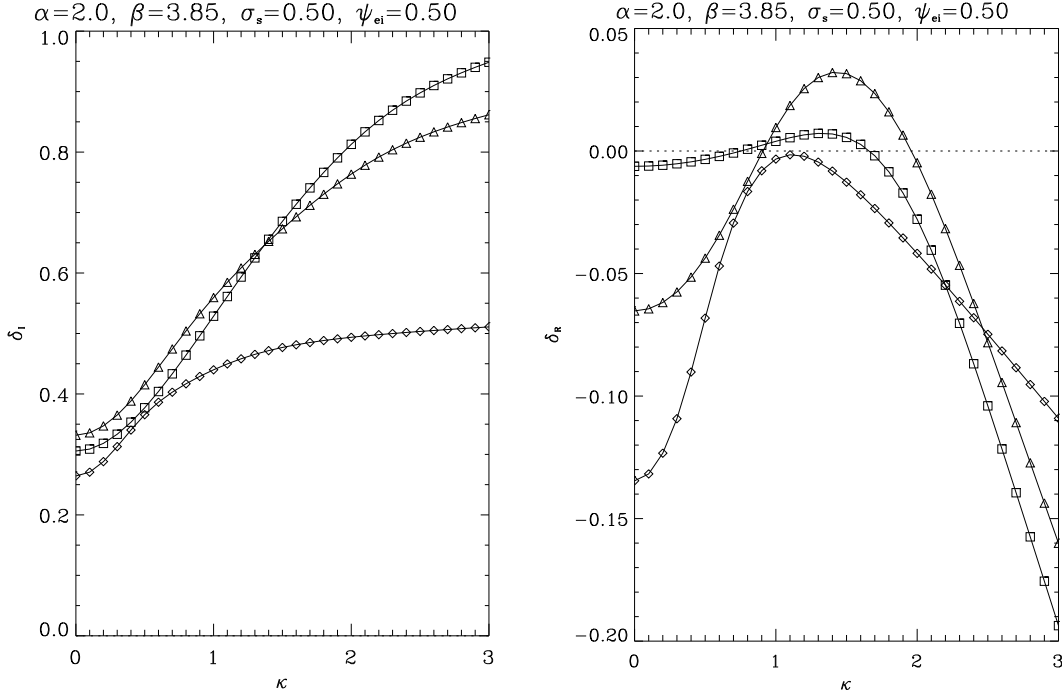


Figure 2. Oscillatory part and stability term of the eigenfrequency for the $n = 1$ mode, with varying transverse wavenumber κ , in the presence of two-temperature effects. Squares, triangles and diamonds represent the bremsstrahlung plus cyclotron cooling cases $\epsilon_s = 0, 1, 100$ respectively.

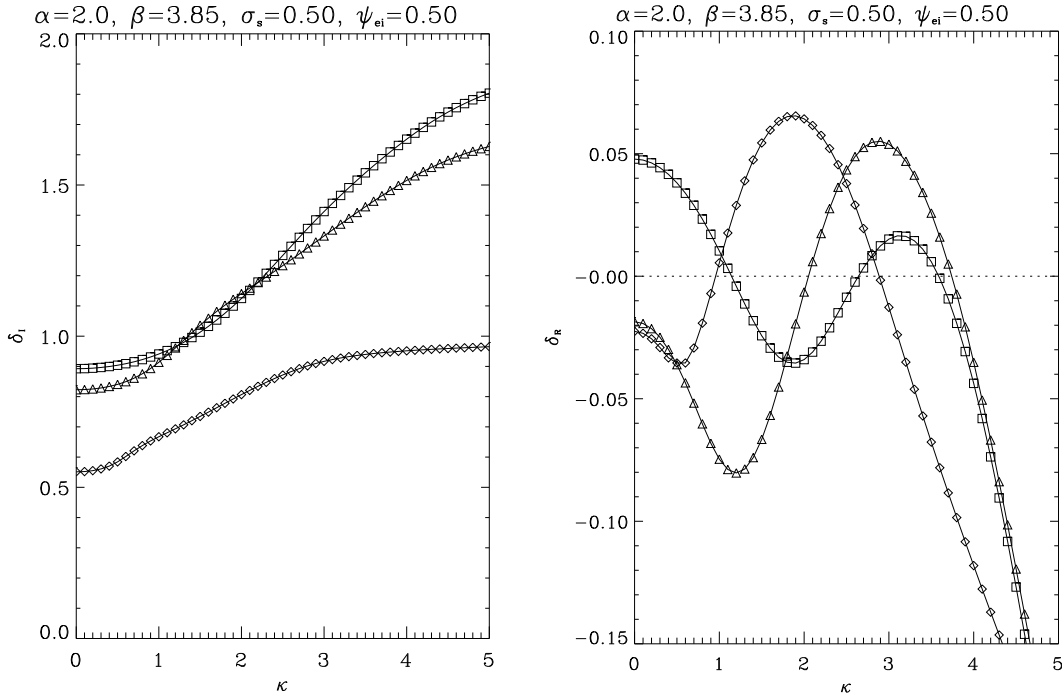


Figure 3. Same as Figure 2 but for the $n = 2$ mode.

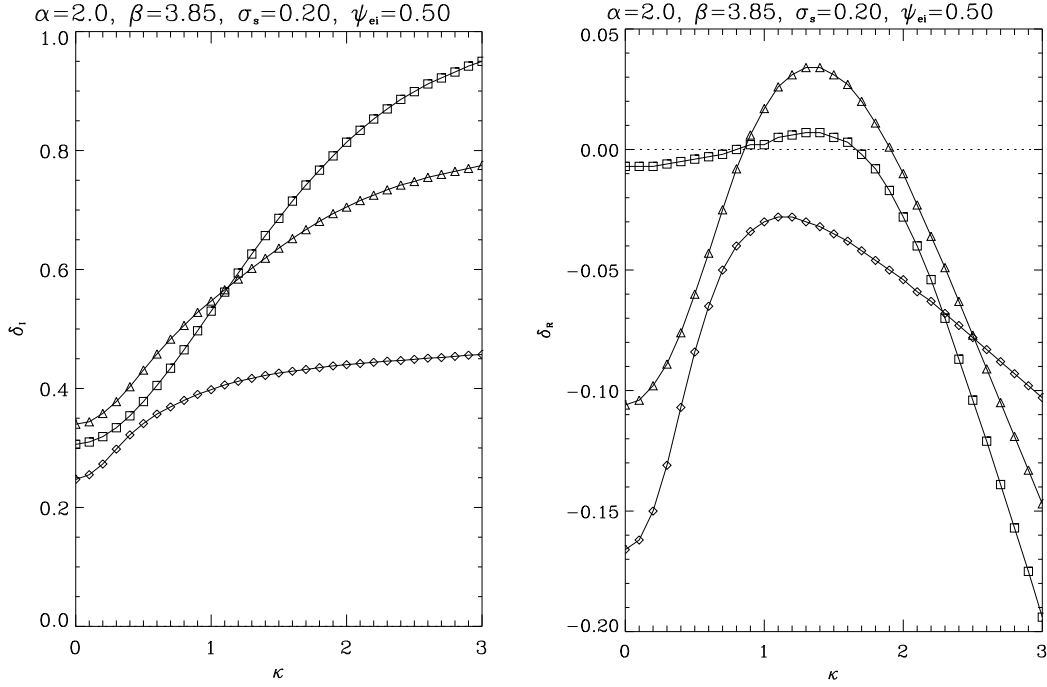


Figure 4. Same as Figure 2 but for the $n = 1$ mode, $\sigma_s = 0.2$, $\psi_{ei} = 0.5$.

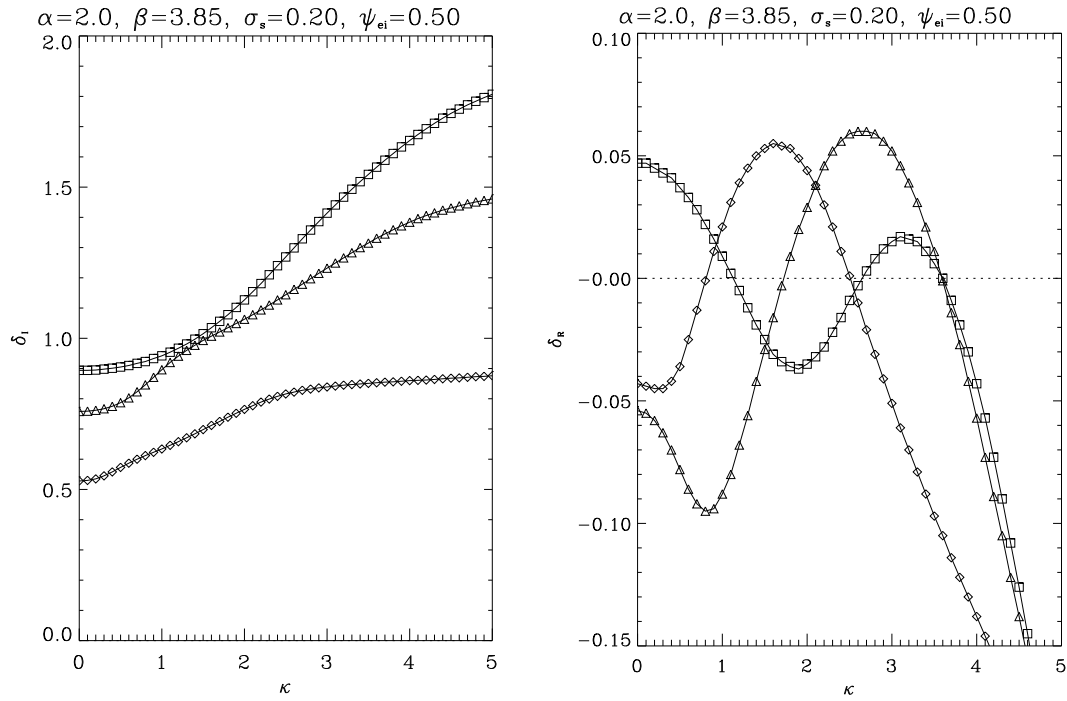


Figure 5. Same as Figure 2 but for the $n = 2$ mode, $\sigma_s = 0.2$, $\psi_{ei} = 0.5$.

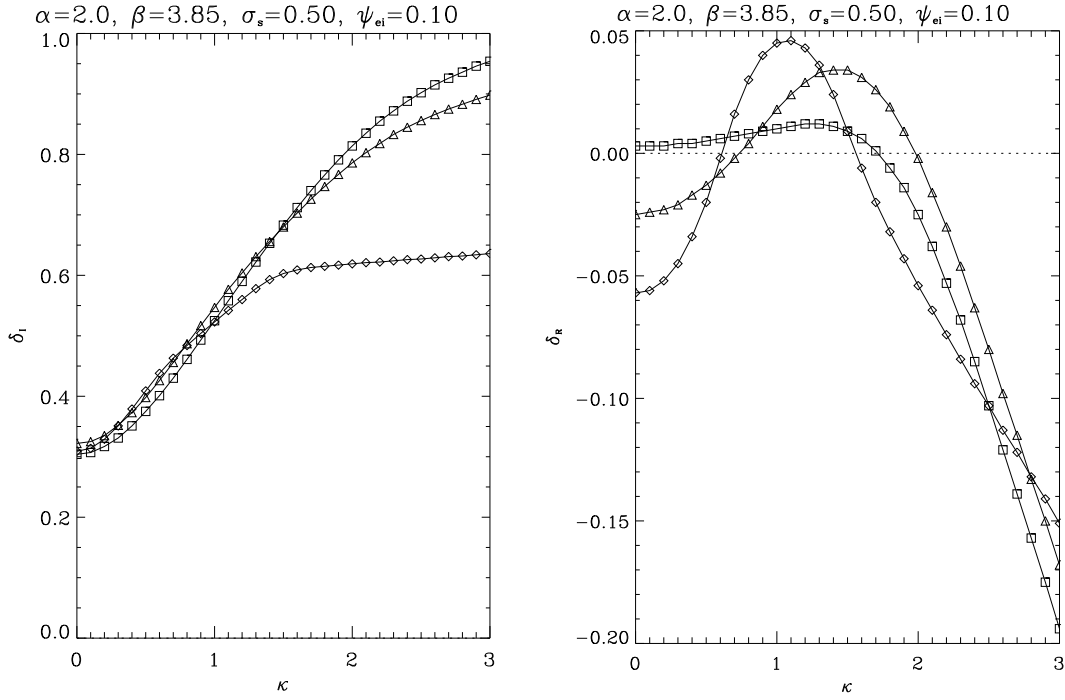


Figure 6. Same as Figure 2 but for the $n = 1$ mode, $\sigma_s = 0.5$, $\psi_{ei} = 0.1$.

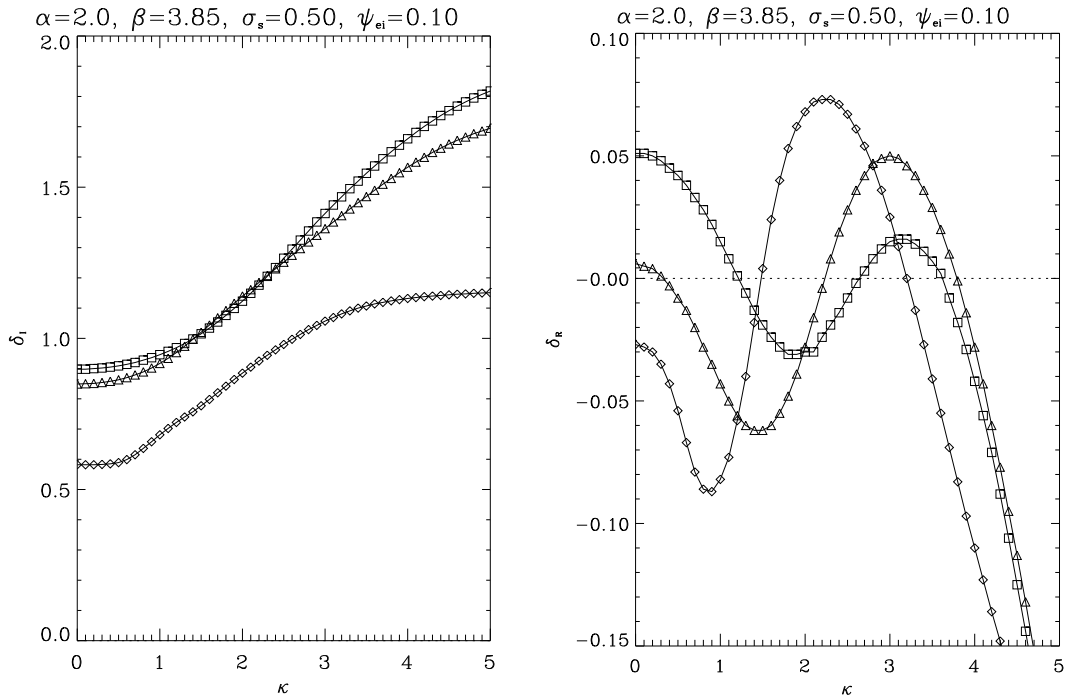


Figure 7. Same as Figure 2 but for the $n = 2$ mode, $\sigma_s = 0.5$, $\psi_{ei} = 0.1$.

the two-temperature flow parameters (σ_s, ψ_{ei}). Except when ϵ_s is very large and σ_s is small, the δ_R of each mode only ever decreases with an increase in ϵ_s .

(ii) The effect of varying the electron-ion coupling ψ_{ei} is insignificant in the bremsstrahlung-cooling dominated regime (ϵ_s small). Decreasing ψ_{ei} , making the electron-ion exchange inefficient, tends to destabilize the accretion column in all modes, and increases the frequency spacing of the modes slightly.

(iii) Varying the ratio of electron and ion pressures at the shock σ_s affects the frequency spacing of the modes in non-simple ways. For some choices of the global parameters a given change in σ_s increases the frequency spacing; in other cases it causes a decrease. Decreasing σ_s usually reduces the instability of modes, and this is accentuated when ϵ_s is high.

(iv) Transverse perturbations yield δ_R maxima in κ that can destabilize modes that are stable to purely longitudinal oscillations. If σ_s is not too small then these maxima may enter the stable regime again for sufficiently great ϵ_s .

5 DISCUSSION

Most previous perturbative analyses of radiative shocks (e.g. Chevalier & Imamura 1982, Bertschinger 1986, Houck & Chevalier 1992, Tóth & Draine 1993, Dgani & Soker 1994) represented the cooling function as a single-power-law term, and set the indices to various values to mimic the presence of different physical cooling processes. Such formulations do not adequately describe systems where more than one cooling process is significant, especially where these processes differ greatly in their innate influences over thermal instability. The realistic interplay between the influences of a stabilizing cooling process and a destabilizing cooling process was explicitly included in Saxton et al. (1997) and Saxton et al. (1998). This condition is retained in the present extended treatment, and by taking the one-temperature limit we recover the earlier results.

Our investigation considers the additional effects of unequal electron and ion temperatures, as in the work of Imamura et al. (1996), which considered accretion onto non-magnetic white dwarfs. Ours combines the two-temperature treatment with the effects of the joint presence of bremsstrahlung and cyclotron cooling. Therefore our analysis is applicable to radiative accretion shocks on white dwarfs in magnetic cataclysmic variables with radiative cooling timescales possibly comparable to or faster than the electron-ion energy exchange.

The accretion column in a mCV is not geometrically extended in the vertical direction (see e.g. Cropper 1990), and the field-aligned flow suffers no transverse mass flux (unlike the case of Dgani & Soker 1994). Our cases of nonzero ϵ_s correspond to magnetic fields much stronger than those investigated by Hujeirat & Papaloizou (1998), and therefore the field can not develop large transverse kinks that would suppress oscillations by the mechanism of Tóth & Draine (1993). The altitude of the shock above the white dwarf surface is negligible compared to the size of the white dwarf, so the variation of gravity in the accretion column, studied by Houck & Chevalier (1992), is unimportant. Therefore we do not investigate effects of non-planar geometry (as in Bertschinger 1986). Transverse perturbations, which are manifest as corrugation of the shock structure and oscillation, are studied, (as in Imamura et al. 1996).

Except when the energy exchange of electrons and ions is very weak, increasing the efficiency of the cyclotron cooling ϵ_s (i.e. strengthening the ambient magnetic field) stabilizes each mode monotonically. The modes stabilize at independent rates in ϵ_s , meaning that some of those modes which are highly unstable in the weak-field regime may actually stabilize at low thresholds of ϵ_s . The detailed behaviour of the mode stabilization in ϵ_s depends on the parameters σ_s and ψ_{ei} .

As in Saxton et al. (1998) the instability of a particular mode does not imply the instability of all higher modes, when more than a single cooling process is significant. This characteristic of competition between cooling processes persists in the general two-temperature and non-longitudinal oscillation cases. If cyclotron cooling is significant relative to bremsstrahlung cooling, the electron-ion exchange process determines the sequence of δ_R , but the frequency spacing of the quantized δ_l sequence depends mainly on ϵ_s . Cases of bremsstrahlung-cooling dominated shocks are similar and their properties are scarcely affected by two-temperature effects.

The basic sequence of mode stabilities in the bremsstrahlung-cooling dominated case has a stable fundamental and each higher mode less stable than its predecessor. Strengthening cyclotron cooling tends to stabilize all the modes, but does so in a fashion that is individual to each mode, so that deviations from the trend develop as ϵ_s increases (especially in the presence of two-temperature effects). For low ϵ_s these stability deviations are slight. For greater ϵ_s , the δ_R sequence of the modes is a less simple pattern depending on the parameters of the shock pressures σ_s and electron-ion exchange ψ_{ei} .

Two-temperature effects dominate the properties of the modes when ϵ_s is very high, and beyond some threshold in ϵ_s , which depends on (σ_s, ψ_{ei}), two-temperature effects have a destabilizing influence. If the electron-ion exchange is sufficiently weak, the exchange process dominates the oscillations and some modes that would be stable at lower ϵ_s become unstable again at higher ϵ_s .

The non-simple order in which the modes are stabilized means that the thermal instability properties of accretion shocks in mCVs are not simply a trivial result of a relationship between oscillatory, cooling and energy exchange timescales. The competing effects must be considered in detail. However we note that our analysis proves modes to be unstable, but does not necessarily prove stability. Minorsky (1962, chapter 14) uses topological and perturbative analytic arguments to consider the general conditions of stability of non-linear oscillatory systems. This issue was also addressed by Lyapunov in his analysis of stability of dynamical systems (Lyapunov 1966, see section 1.5.3, Leipholz 1970 for another treatment of Lyapunov's theorems on stability). In summary, the linear terms dominate in the limit of small amplitudes, i.e. every mode that is linearly unstable remains unstable in a full non-linear treatment, although higher-order contributions may cause a stable limit cycle at larger amplitudes.

6 CONCLUSIONS

We investigated plane-parallel radiative shocks in which bremsstrahlung and cyclotron cooling may be fast compared with electron-ion energy exchange. Parameters and boundary conditions are chosen to be appropriate for accretion onto the surface of a magnetic white dwarf. The cooling function was an explicit sum of contributions from thermal bremsstrahlung (which destabilizes the flow) and cyclotron cooling (which has a stabilizing tendency).

The relative efficiency of the cyclotron emission ϵ_s is varied. Stability of the shock to longitudinal and non-longitudinal perturbations was investigated. The ratio of electron and ion pressures at the shock σ_s , and the rate of electron-ion energy exchange ψ_{ei} were also varied. Variations of the exchange, pressure and cooling parameters, $(\sigma_s, \psi_{ei}, \epsilon_s)$, affect the stability and frequency of each mode in a manner that is individual to the mode and the conditions of the stream. Increasing ϵ_s increases the stability of each mode, until a threshold value in ϵ_s is exceeded. Beyond this point, increasing ϵ_s destabilizes a mode slowly. This threshold is very high except when ψ_{ei} is very small.

The introduction of unequal electron and ion temperatures has little effect on the modes of a bremsstrahlung-cooling dominated accretion column. In these cases, the higher harmonics tend to be less stable to oscillations. When bremsstrahlung and cyclotron cooling are comparable in strength, the pattern of the modes' stabilities becomes less regular, and two-temperature effects tend to stabilize the shock. For a cyclotron-cooling dominated shock all of the modes are stable in the single-temperature limit, but introduction of two-temperature effects can make them less stable. In some cases of small ψ_{ei} one or more of the lower modes may be unstable even for high ϵ_s . Unlike the bremsstrahlung emission, cyclotron cooling is strongest near the shock, where the difference of electron and ion temperatures is greatest. Therefore the slightest presence of two-temperature effects means that the stability of a cyclotron-cooling dominated shock is dominated by the energy exchange between the two fluid components rather than the cooling function.

Many cases exist where the mode n is unstable while the mode $n + 1$ is stable, and some higher modes are unstable. This is a general characteristic of radiative shocks with competing stabilizing and destabilizing cooling processes, and is preserved in the generalization to conditions with two-temperatures and non-longitudinal perturbations.

The oscillatory parts of the dimensionless eigenfrequencies δ_1 follow a sequence which is approximately regular and linear. In the single-temperature case this sequence resembles the modes of a pipe open at one end: $\delta_1 \approx \delta_{1O}(n - 1/2) + \delta_C$. When two-temperature effects are present the limit of large ϵ_s causes the frequencies to approach quantization like a doubly-open pipe $\delta_1 \approx \delta_{1O}n$, because of the fixed velocity condition at the white dwarf surface becomes less significant than the electron-ion thermal disparity throughout the column. The frequency spacing of the modes, δ_{1O} , always decreases as ϵ_s increases, but tends to increase when the electron-ion exchange is weaker. The frequency offset δ_C is small for low ϵ_s and it generally increases with increasing ϵ_s ; in the limit of cyclotron cooling and two-temperature dominance the offset approaches $\delta_C \rightarrow \frac{1}{2}\delta_{1O}$, giving the doubly-open pipe behaviour.

Introducing transverse perturbations can destabilize modes that are stable to purely longitudinal perturbations, except when cyclotron cooling dominates or two-temperature effects are strong. The modes become non-unique in δ_1 , for different κ . In the limit of large κ all modes are stable with oscillatory parts quantized like a doubly-open pipe $\delta_1 \propto n$, regardless of the manner of their quantization under the same parameters in the absence of transverse perturbations. Each mode has a number of instability maxima in κ , and these maxima evolve as the parameters $(\sigma_s, \psi_{ei}, \epsilon_s)$ change. When the pressure ratio at the shock σ_s is small, the maxima of δ_R are stabilized at lower ϵ_s . When the electron-ion exchange is weak (ψ_{ei} is small), the maxima may continue to destabilize at high ϵ_s .

7 ACKNOWLEDGEMENTS

KW acknowledges the support from the Australian Research Council through an ARC Australian Fellowship.

REFERENCES

- Aizu, K., 1973, *Prog. Theor. Phys.*, 49, 1184
 Bertschinger, E., 1986, *ApJ*, 304, 154
 Chanmugam G., Langer, S. H., Shaviv, G., 1985, *ApJ*, 299, L87
 Chevalier, R. A., Imamura, J. N., 1982, *ApJ*, 261, 543
 Cropper, M., 1990, *Sp. Sci. Rev.*, 54, 195
 Cropper, M., Wu, K., Ramsay, G. Kocabiyik, A., 1999, *MNRAS*, 306, 684
 Dgani, R., Soker, N., 1994, *ApJ*, 434, 262
 Gaetz, T. J., Edgar, R. J., Chevalier, R. A., 1988, *ApJ*, 329, 927
 Falle, S. A. E. G., 1975, *MNRAS*, 172, 55
 Falle, S. A. E. G., 1981, *MNRAS*, 195, 1011
 Houck, J. C., Chevalier, R. A., 1992, *ApJ*, 395, 592
 Hujerir, A., & Papaloizou, J. C. B., 1988, *A&A*, 340, 593
 Imamura, J. N., 1985, *ApJ*, 296, 128
 Imamura, J. N., Wolff, M. T., 1990, *ApJ*, 355, 216
 Imamura, J. N., Wolff, M. T., Durisen, R. H., 1984, *ApJ*, 276, 667
 Imamura, J. N., Aboasha, A., Wolff, M. T., Wood, K. S., 1996, *ApJ*, 458, 327

- Innes, D. E., Giddings, J. R., Falle, S. A. E. G., 1987a, MNRAS, 224, 179
Innes, D. E., Giddings, J. R., Falle, S. A. E. G., 1987b, MNRAS, 226, 67
King, A. R., Lasota, J. P., 1979, MNRAS, 188, 653
Lamb, D. Q., Masters, A. R., 1979, ApJ, 234, L117
Langer, S. H., Chanmugam, G., Shaviv, G., 1981, ApJ, 245, L23
Langer, S. H., Chanmugam, G., Shaviv, G., 1982, ApJ, 258, 289
Leipholtz, H., 1970, *Stability Theory: An Introduction to the Stability of Dynamic Systems and Rigid Bodies*, Academic Press, New York
Lyapunov, A. M., 1966, *Stability of Motion*, Academic Press, New York
Melrose, D. B., 1986, *Instabilities in Laboratory and Space Plasmas*, Cambridge University Press, Cambridge
Minorsky, N., 1962, *Nonlinear Oscillations*, Van Nostrand, Princeton
Rybicki, G. B., Lightman, A. P., 1979, *Radiative Processes in Astrophysics*, John Wiley & Sons, New York
Saxton, C. J., 1999, PhD Thesis, University of Sydney, Australia.
Saxton, C. J., Wu, K., Pongracic, H., 1997, Publ. Astr. Soc. Australia, 14, 164
Saxton, C. J., Wu, K., Pongracic, H., Shaviv, G., 1998, MNRAS, 299, 862
Tóth, G., Draine, B. T., 1993, ApJ, 413, 176
Warner, B., 1995, *Cataclysmic Variable Stars*. Cambridge Univ. Press, Cambridge, p.256
Wolff, M. T., Gardner, J., Wood, K. S., 1989, ApJ, 346, 833
Wu, K., 1994, Proc. Astr. Soc. Australia, 11, 61
Wu, K., Chanmugam, G., Shaviv, G., 1992, ApJ, 397, 232
Wu, K., Chanmugam, G., Shaviv, G., 1994, ApJ, 426, 664
Wu, K., Pongracic, H., Chanmugam, G., Shaviv, G., 1996, Publ. Astron. Soc. Aust., 13, 93